Inelastic neutron scattering in tetragonal $KNbO_3$

M. D. Fontana
Laboratoire de Physique des Milieux Condensés, Université de Metz, Ile du Saulcy, 57000 Metz, France

G. Dolling
Atomic Energy of Canada Limited, Chalk River, Ontario, Canada, KOJ 1JO

G. E. Kugel and C. Carabatos
Laboratoire de Physique des Milieux Condensés, Université de Metz, Ile du Saulcy, 57000 Metz, France

(Received 18 April 1979)

Inelastic neutron scattering experiments in tetragonal $KNbO_3$ show a high anisotropy in some regions of the phonon dispersion relation and the existence of strong one-dimensional intercell correlations between atomic motions along the [100] and [010] directions, in agreement with x-ray diffuse-scattering measurements in the same phase. The transverse phonon modes propagating *normally* to these directions of strong correlations, that is, with polarization vectors parallel to them, are relatively soft, not only near the zone center but all the way to the zone boundary. Comparison of these results with the Raman, neutron, and x-ray data obtained in the other phases suggests a description of the ferroelectric phase transition mechanism in $KNbO_3$ in terms of soft modes and dynamic correlations in each phase.

I. INTRODUCTION

Potassium niobate, $KNbO_3$, has been the object of many investigations involving Raman, neutron, and x-ray scattering, principally in its room-temperature orthorhombic phase. Above the transition temperature of 435 °C, $KNbO_3$ is an archetypal cubic perovskite crystal belonging to the O_h^1 space group. It undergoes three different successive ferroelectric phase transitions with decreasing temperature. First, it becomes tetragonal (space group C_{4v}^1) with appearance of a spontaneous polarization P_s along the [001] direction; then at 215 °C it becomes orthorhombic (space group C_{2v}^{14}) with P_s parallel to the [101] pseudocubic axis, and finally rhombohedral (space group C_{3v}^1) at −50 °C with P_s along the [111] pseudocubic axis.

The structure of each phase has been determined by Hewat[1] using the neutron powder profile refinement technique. By means of x-ray diffraction experiments, Comes *et al.*[2] observed an unexpectedly strong diffuse scattering between reciprocal-lattice points in each phase except for the rhombohedral one. The scattering intensity is approximately constant between two Bragg points and temperature independent between two transitions but it is modified at each phase transition. In the cubic phase three sets of planes normal to the cubic axes ⟨100⟩ are observed; in the tetragonal phase the (001) planes disappear; in the orthorhombic phase only the (010) planes are observed; these diffuse sheets disappear at the rhombohedral phase transition.

From these results, Comes *et al.*[2] suggested that the transitions are of the order-disorder type and all the phases but the rhombohedral one are intrinsically disordered. This disorder results from several possible statistical orientations of the "central" Nb ion along different ⟨111⟩ directions; the off-center positions of Nb are correlated along lines parallel to the cubic axes. These correlation chains could give rise to the observed planes of diffuse scattering.

This description, based on the existence of a local static disorder, differs from the soft-mode concept previously developed by Cochran[3] in connection with displacive phase transitions. But Hüller[4,5] has shown that it is not necessary to assume a disorder model to explain the diffuse streaks and that a strong anisotropy of the soft-mode branch can give the same effect.

In an earlier paper[6] we discussed the contribution of the transverse acoustic and optic B_1 and B_2 modes to the orthorhombic-tetragonal and to the orthorhombic-rhombohedral phase transitions, respectively. Here we report the first inelastic neutron scattering experiments on single-domain $KNbO_3$ crystals in the tetragonal phase; our results are compared with those obtained by x-ray and neutron diffraction in all phases and with analogous results for other perovskites.

We conclude by suggesting a description of phase transitions based on the soft-mode theory which ac-

counts for the observation of diffuse-scattering planes and of the anisotropy of the phonon dispersion relation.

II. STRUCTURE AND SYMMETRY

Figure 1 shows the tetragonal unit cell, with atomic positions relative to the cubic origin of coordinates. The parameters of the cell and the δ quantities which measure the atomic displacements from the cubic positions are given in Table I.[1]

The Brillouin zone with the high-symmetry directions Δ, Σ, and Λ is shown in Fig. 1.

The vibrational modes are classified by assigning them to irreducible representations of the space group of the crystal. They are tabulated in the Appendix together with the form of the corresponding symmetrized vectors. The compatibility relations with the zone-center modes are also given in the Appendix.

The space group of the three ferroelectric phases are subgroups of the O_h^1 cubic group, but they are not subgroups of one another. Thus the ferroelectric cells can be constructed by small distortions of the cubic cell. Since these distortions are very small, it is convenient to refer all axes and directions back to "pseudocubic" axes. The vibrational modes can also be grouped according to the cubic modes from which they are derived. In Table II we describe the compatibility relations between modes belonging to different phases. For example, in the cubic phase, at the long-wavelength limit ($q \simeq 0$) the modes transform as the four $F_{1u}+F_{2u}$ irreducible representations of the point group O_h. The long-range electrostatic forces split each triply degenerate F_{1u} mode into a doubly degenerate transverse mode and a singlet longitudinal mode. The F_{1u} modes are polarized along the three equivalent cubic axes. The

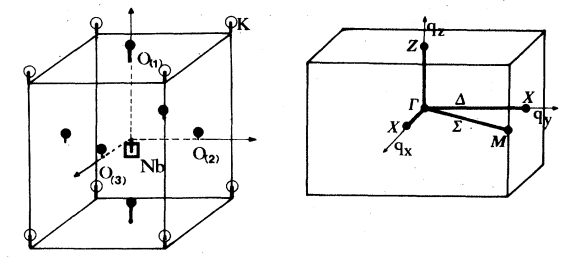

□	Nb	0	0	δ[Nb]
○	K	$\frac{1}{2}a$	$\frac{1}{2}a$	$\frac{1}{2}c+\delta[K]$
●	$O_{(1)}$	0	0	$\frac{1}{2}c+\delta(O_{(1)})$
	$O_{(2)}$	0	$\frac{1}{2}a$	$\delta(O_{(2)})$
	$O_{(3)}$	$\frac{1}{2}a$	0	$\delta(O_{(3)})$

Γ	0	0	0
Z	0	0	$\frac{\pi}{c}$
X	$\frac{\pi}{a}$	0	0
	0	$\frac{\pi}{a}$	0
M	$\frac{\pi}{a}$	$\frac{\pi}{a}$	0

FIG. 1. Unit cell and Brillouin zone in tetragonal $KNbO_3$.

TABLE I. Parameters of the tetragonal cell [Hewat (Ref. 1)].

$a = 3.997$ Å	$c = 4.063$ Å
$\delta(K) = -0.014 \pm 26$ Å	$\delta(Nb) = 0.063$ Å
$\delta(O_{(1)}) = -0.117 \pm 4$ Å	$\delta(O_{(2)}) = \delta(O_{(3)}) = -0.099$ Å

lowest frequency TO F_{1u} mode is called the ferroelectric mode.

At the cubic-tetragonal phase transition, each cubic F_{1u} mode transforms according to the A_1+E irreducible representations of the point group C_{4v}, where E is a doubly degenerate representation. The F_{2u} mode transforms as the B_1+E irreducible representations. The A_1 modes are polarized along the [001] axis, the E modes along [100] and [010] axes. In the orthorhombic phase, each F_{1u} mode transforms according to the $A_1+B_1+B_2$ irreducible representations, while the modes $A_1+A_2+B_1$ are derived from the cubic F_{2u} mode. The A_1, B_1, and B_2 modes are polarized, respectively, along the [101], [10$\bar{1}$], and [010] axes defined in the pseudocubic system.

We continue to call "ferroelectric" the modes derived from the cubic ferroelectric F_{1u} mode.

III. EXPERIMENTS

The samples of $KNbO_3$ were prepared by G. Metrat with a modified floating-crystal method described in a recent paper.[6]

The orthorhombic-tetragonal phase transition is accomplished in a special furnace and great care must be exercised to obtain a monodomain crystal in the tetragonal phase. First, in order to avoid cracks which can appear between different phase boundaries, we applied a thermal gradient such that *one* new phase boundary appears in a corner of the sample and develops progressively along the gradient. Second, in order to ensure a complete domain alignment parallel to the future ferroelectric axis, a specially oriented electric field is applied between the faces. By this method we succeeded in obtaining a 95% monodomain crystal.

The inelastic neutron scattering experiments were performed on the N5 triple-axis spectrometer at the Chalk River NRU reactor, using the "constant Q" technique with a variable neutron incident energy and fixed scattered neutron energies, E/h, of 6.3, 7.5, or 9 THz. We used the (113) plane of Si and the (002) plane of Cu as monochromator and analyzer, respectively. In various sets of experiments, either the (00l) and ($0k$ 0) planes of the $KNbO_3$ sample were aligned parallel to the horizontal scattering plane of the spectrometer, in order to measure the dispersion

TABLE II. Compatibility relations between modes of the cubic phase and of the tetragonal and orthorhombic phases.[a]

Wave vector	Cubic	Tetragonal	Orthorhombic
$\vec{q}=(0,0,0)$	$4\Gamma_{15}^{(3)}(F_{1u}^{(3)})$ $1\Gamma_{25}^{(3)}(F_{2u}^{(3)})$	$4[\Gamma_1(A_1)+\Gamma_5^{(2)}(E^{(2)})]$ $1[\Gamma_3(B_1)+\Gamma_5^{(2)}(E^{(2)})]$	$4[\Gamma_1(A_1)+\Gamma_3(B_2)+\Gamma_4(B_1)]$ $[\Gamma_1(A_1)+\Gamma_2(A_2)+\Gamma_4(B_1)]$
$\vec{q}=(\zeta,0,0)$	$4\Delta_1$ Δ_2 $5\Delta_5^{(2)}$	$4\Delta_1$ Δ_1 $5(\Delta_1+\Delta_2)$	$4\tau_1$ τ_1 $5(\tau_1+\tau_2)$
$\vec{q}=(0,\zeta,0)$	$4\Delta_1$ Δ_2 $5\Delta_5^{(2)}$	$4\Delta_1$ Δ_1 $5(\Delta_1+\Delta_2)$	$4\Delta_1$ Δ_2 $5(\Delta_1+\Delta_2)$
$\vec{q}=(0,0,\zeta)$	$4\Delta_1$ Δ_2 $5\Delta_5^{(2)}$	$4\Lambda_1$ Λ_2 $5\Lambda_5^{(2)}$	
$\vec{q}=(\zeta,\zeta,0)$	$5\Sigma_1$ Σ_2 $5\Sigma_3$ $4\Sigma_4$	$5\Sigma_1$ Σ_2 $5\Sigma_2$ $4\Sigma_1$	
$\vec{q}=(\zeta,0,\bar{\zeta})$	$5\Sigma_1$ Σ_2 $5\Sigma_3$ $4\Sigma_4$		$5\Sigma_1$ Σ_2 $5\Sigma_1$ $4\Sigma_2$
$\vec{q}=(\zeta,0,\zeta)$	$5\Sigma_1$ Σ_2 $5\Sigma_3$ $4\Sigma_4$		$5\Lambda_1$ Λ_2 $5\Lambda_4$ $4\Lambda_3$

[a]The group-theoretical results in the cubic and orthorhombic phases are given by Cowley (Ref. 24) and Currat *et al.* (Ref. 14), respectively. The notation we use is that of Kovalev (Ref. 25); for the Γ point the chemical notation is included in parentheses. The notation of the high-symmetry directions in each phase is that of Bradley and Cracknell (Ref. 26); but for the [100] direction of the orthorhombic cell we use the general τ_i notation.

curves in the high-symmetry directions. Some typical neutron groups are shown in Fig. 2.

IV. RESULTS

A. Tetragonal phase

1. Δ direction [$\vec{q}\parallel(\zeta,0,0)$]

Group theory leads to 5 branches of Δ_2 symmetry and 10 of Δ_1 symmetry. The Δ_2 modes are strictly transverse and polarized along the [010] direction when propagating along the [100] axis. The Δ_1 phonons are neither purely transverse nor longitudinal; nevertheless we can have an approximate description for small wave vectors by using the compatibility relations with the zone-center modes. The Δ_2 phonons were measured around the (0,4,0), (0,3,0), and (1,4,0) reciprocal-lattice points, i.e., in pure or nearly pure transverse configurations. For the Δ_1 phonons, data were collected around the (4,0,0), (1,0,4), and (0,0,4) reciprocal-lattice points. The Δ_1 and Δ_2 dispersion curves obtained are shown in Fig. 3; the shapes of the Δ_1 and Δ_2 branches are seen to be completely different.

a. Δ_2 phonons. The TA and lowest frequency TO phonons are not well defined; indeed, since these branches belong to the same representation, they interact strongly, giving rise to anticrossing of the branches and broadening of the neutron groups. The frequency of the Δ_2 (TA) mode is anomalously low in the Brillouin zone and is essentially constant between $q=0.2$ and the zone boundary. The frequency of the lowest Δ_2 (TO) branch is also quite low over the entire zone.

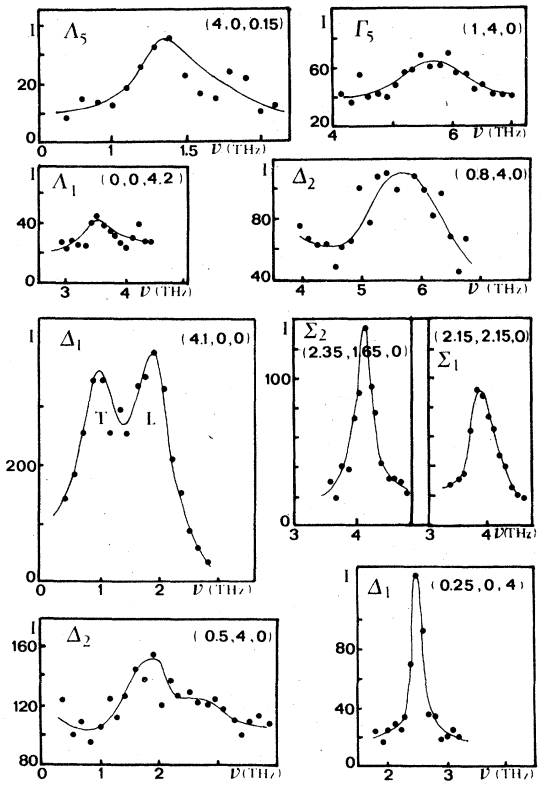

FIG. 2. Typical neutron groups in tetragonal $KNbO_3$. The intensity of counting, I, is in arbitrary units. The symmetry and the momentum transfer Q are specified in each group.

The presence of a low-frequency zone-center TO mode of E symmetry is consistent with the high value of the corresponding ϵ_a dielectric constant (along the [100] axis) measured by Wiesendanger.[7]

A flat Δ_2 (TO) branch is measured at about 6 THz; an increasing broadening of the peaks with increasing wave vector can be seen.

b. Δ_1 *phonons.* In contrast to the Δ_2 phonons, the Δ_1 are well defined and their behavior is quite normal. The neutron groups are well resolved and no broadening is observed. The pseudo-TA and -LA branches have a normal $\vec{q}$ dependence, i.e., the phonon energy increases with increasing wave vector. A flat pseudo-LO branch is reported between 6 and 7 THz.

A low-frequency zone-center TO mode of A_1 symmetry is not observed. Our recent Raman scattering data place a A_1 mode frequency at 280 cm^{-1}.[8] Thus it seems that the highest Δ_1 mode measured by neutron scattering is a pseudo-TO branch corresponding to this A_1 mode for $q=0$. This shows that the ϵ_c dielectric constant along the [001] direction is much lower than the ϵ_a dielectric constant, in agreement with Wiesendanger's result.[7] Moreover, this proves that the [001] component of the ferroelectric cubic mode is "stiffened" during the transition, that is, its frequency increases.

2. Σ direction [$\vec{q} \parallel (\zeta, \zeta, 0)$]

As indicated in Appendix the Σ_1 and Σ_2 modes are not purely transverse or longitudinal. Data were collected only in the (2,2,0) Brillouin zone. The results are presented in Fig. 4.

The behavior of the pseudo-TA (Σ_2) and pseudo-LA (Σ_1) branches is very analogous to that of the corresponding Δ_1 branches. The Σ_2 pseudo-TO branch frequency is low only for small wave vectors, and increases rapidly with increasing q. We note that in this direction the phonons are well defined.

3. Λ direction [$\vec{q} \parallel (0, 0, \zeta)$]

In this direction, the Λ_1 and Λ_2 branches are strictly longitudinal and the Λ_5 are doubly degenerate and

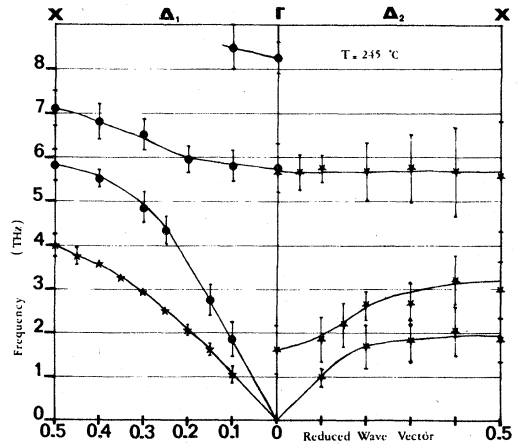

FIG. 3. Dispersion curves of Δ_1 and Δ_2 symmetry in tetragonal $KNbO_3$.

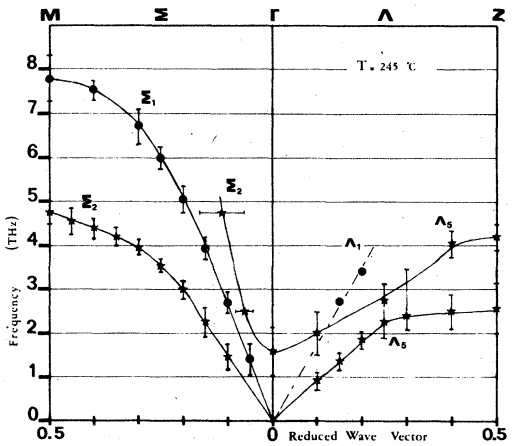

FIG. 4. Dispersion curves of Σ and Λ symmetry in tetragonal $KNbO_3$.

transversely polarized. They are shown in Fig. 4.

The slope of the LA Λ_1 branch is similar to that of Λ_1. The behavior of the lowest TO and TA Λ_5 branches looks very similar to the corresponding Δ_2 modes: the phonon peaks are not well defined; broadening and anticrossing phenomena are observed. We note that the flat region of the Λ_5 (TA) branch is more restricted than for the corresponding Δ_2, because the Brillouin zone is smaller in this direction.

4. Summary of the results in the tetragonal phase

Our neutron data show a large splitting between the zone-center modes deriving from the ferroelectric cubic F_{1u} mode: the [001] component (A_1 mode) has a frequency much higher than that of the [100] or [010] component (doubly degenerate E mode), in agreement with the values of the corresponding dielectric constants ϵ_c and ϵ_a $(=\epsilon_b)$.

The dispersion relations of the TA and ferroelectric TO branches are very anisotropic; the phonon frequencies are very low in the whole Brillouin zone when polarized along the [100] or [010] directions. For other mode polarization directions the phonon frequency rises steeply with increasing wave vector and the shapes of the branches appear normal. The TA and ferroelectric TO modes of Δ_1 and Σ_2 symmetry and of mixed polarization show a similar behavior. Nevertheless, we note that while the TA branches appear similar, the ferroelectric Δ_1 and Σ_2 modes are very different. They correspond respectively to a "stiffened" and a "soft" mode at the zone center.

In the same way, the phonon interaction is very dependent on mode symmetry. For the Δ_2 and Λ_5 symmetry, the TA and lowest TO branches belonging to the same irreducible representation interact strongly and display significant damping. For the Δ_1 and Σ_2 symmetry, such effects are not observed.

These results may be compared with the x-ray patterns where a strong diffuse scattering is observed in the (100) and (010) planes.[2]

In order to have a comparative discussion including all phases, it is now useful to recall results obtained by various authors in the other phases.

B. Results in the other phases

1. Cubic phase

Only a few data are available in the cubic phase. Nunes *et al.*[9] have measured the dispersion relation of the TA modes in the [100] and [110] directions. The Δ_5 (TA) phonons polarized along the [010] direction are broad, in contrast with the Σ_3 (TA) modes polarized along the [1$\bar{1}$0] direction, which are well defined. A striking feature is the presence of diffuse scattering associated with overdamped modes having a polarization vector parallel to the ⟨100⟩ directions. The x-ray patterns show an intense diffuse scattering, very sharply localized in the {100} planes.[2]

2. Orthorhombic phase

The Raman scattering results of various authors[10–13] are in reasonable agreement. They show a high anisotropy of the zone-center ferroelectric modes; the frequencies of the stiffened components (A_1 and B_1 modes) are much higher than that of the [010] component (B_2 mode). The inelastic neutron scattering results of Currat *et al.*[14] and of Perry *et al.*[15] indicate a high anisotropy of the TA branch at large wave vector q. This branch is flat for a mode propagating in the (010) plane and at low frequency when polarized along the [010] direction. However, the ferroelectric TO branch has a quite normal $\vec{q}$ dependence; when polarized along the [010] axis, its frequency is low only for small wave vectors and then increases with q. In contrast with the tetragonal and cubic phases, the phonons are well defined and no strong interaction is observed. The x-ray diffraction[2] shows a diffuse scattering localized in the (010) planes.

3. Rhombohedral phase

Dispersion curves have not yet been determined in this phase. However, the absence of strong Raman scattering at low frequencies[13,16] shows that the final component of the ferroelectric mode has stiffened. This is also indicated by the x-ray results which display no planes or lines of diffuse scattering.

V. DISCUSSION

1. Zone-center modes

The comparison between the results obtained in the three ferroelectric phases show that the lowest frequency cubic F_{1u} mode is affected to the greatest extent by the successive ferroelectric phase transitions. At each transition, this mode is split into soft and stiffened components. Since the soft optic mode is polar, it can give rise to a macroscopic polarization at each transition.

The phase transitions in $KNbO_3$ are thus of the displacive type, with the condensation of a soft component of the ferroelectric F_{1u} mode at each transition: the atomic vibrations of this mode "freeze" into the static displacements and thus produce a cell distortion and a permanent dipole component along their polarization.

2. *Distribution of x-ray scattering intensity and phonon dispersion curves*

The distribution of the scattered x-ray intensity in reciprocal space and the dispersion relation of the TA and ferroelectric TO modes are strongly anisotropic in the three high-temperature phases. These properties are of course correlated. Indeed, the intensity of x-rays scattering by phonons is given, in the harmonic approximation, by

$$I(Q) = Nk_B T \sum_j \frac{|F_i(\vec{Q})|^2}{\omega^2(\vec{q},j)} ,$$

where

$$F_i(\vec{Q}) = \sum_\kappa f_\kappa \frac{\vec{Q}\cdot\vec{e}(\kappa,q,j)}{m_\kappa^{1/2}} \exp i\vec{Q}\cdot\vec{r}_\kappa$$

is the inelastic structure factor for mode j, $\vec{Q}=\vec{q}+\vec{\tau}$ is the scattering vector, $\vec{e}(\kappa,\vec{q},j)$ is the eigenvector of the κth atom of the j mode, and f_κ is the atomic form factor. It is clear that if the eigenvector is parallel to the momentum transfer Q, and if the mode frequency is low, then we may expect high scattering intensity in appropriate regions of reciprocal space. Hence the sharp streaks observed by x-ray diffraction experiments are associated with atomic motions of low frequency and large amplitude in the direction normal to the plane of the diffuse scattering. The intensity of the streaks remains relatively constant between two Bragg points; this is in agreement with the presence of a flat transverse mode dispersion surface and with slowly varying eigenvectors in certain directions. Thus the anisotropy of the distribution of the x-ray scattering intensity is a direct consequence of the anisotropy of the dispersion surface of the TA and ferroelectric TO modes. For example, in the tetragonal phase, the Δ_2 and Λ_5 low branches polarized along the [010] axis contribute to the (010) diffuse planes. These branches are relatively flat and the direction of the corresponding eigenvector remains constant from the zone center to the zone boundary (see Appendix). On the other hand, the Σ_2 TO branch is soft only for small wave vectors, its frequency subsequently rising steeply with $\vec{q}$, so that no extra intensity is observed in the diagonal planes.

3. *Correlations and soft modes*

The observation of diffuse planes and of low frequency, flat branches demonstrates the presence of strong one-dimensional correlations between the motions of atoms along the ⟨100⟩ axes. Slater[17] long ago and Hüller[5] more recently have shown the importance of polarization effects in perovskite crystals. By analogy, we suggest that the strong correlations of the atomic displacements along the ⟨100⟩ directions are due to linear dipole-dipole forces in these directions favored by the sequence of positive Nb and negative O ions.

Anomalies such as high anisotropy of the TA and TO branches or strong diffuse scattering disappear with the condensation of the last soft component of the ferroelectric mode in the rhombohedral phase. Moreover, we note that the correlations, which are responsible for these anomalies, are directed along the soft-mode eigenvector in each phase. Thus all these anomalies and correlations are related to the phase transition mechanisms and to the ferroelectric properties. The correlations are not between static positions of atoms[2] but between the dynamical vibrations; they are the direct cause of the appearance of ferroelectricity and explain the various anomalous properties of $KNbO_3$.

As in the case of other crystals of the $BaTiO_3$ type, we can assume that the soft mode consists of a vibration of the central Nb ion against the oxygen octahedron; the motion of the niobium atom, the heaviest and probably the least strongly bound atom in the crystal, is the most important. The Nb atoms oscillate with large amplitudes and with strong correlations between cells along the ⟨100⟩ axes. In the cubic phase, for example, there are three linear correlation chains Nb-O-Nb directed along the three cubic axes.

4. *Description of the phase transitions*

The low frequency of a particular mode is a consequence of the near cancellation of competing forces: along the ⟨100⟩ correlation directions, the long-range Coulomb forces are enhanced by polarization effects and tend to cancel the short-range forces. In the course of this soft mode the atoms are displaced along the ⟨100⟩ directions and there is little or no restoring force to bring them back: the crystal becomes unstable against this mode of vibration. At the transition, the ferroelectric soft mode condenses out into static displacements determined by the eigenvector direction, leading to a spontaneous electric polarization along this direction, and a simultaneous elongation of the cell.

In the cubic phase, the Nb atoms are correlated along the three equivalent ⟨100⟩ cubic directions and the "ferroelectric" mode has three soft components polarized along these axes. The branches corresponding to these atomic motions along the correlation directions are of low frequency, and an intense x-ray scattering is visible in the three sets of {100} planes of reciprocal space. At the cubic-tetragonal phase transition, the unstable soft mode

TABLE III. Soft modes in various phases and directions.

	Cubic	Tetragonal	Orthorhombic	Rhombohedral
[100] correlation direction or soft-mode polarization [(100) diffuse planes]	Γ_{15} (F_{1u}) $\Delta_5^{(2)}$ $[\vec{q}\parallel(0,\zeta,0)]$ or $[\vec{q}\parallel(0,0,\zeta)]$ Σ_4 $[\vec{q}\parallel(0,\zeta,\zeta)]$	Γ_5 (E) Δ_2 $[\vec{q}\parallel(0,\zeta,0)]$ $\Lambda_5^{(2)}$ $[\vec{q}\parallel(0,0,\zeta)]$		
[010] correlation direction or soft-mode polarization [(010) diffuse planes]	Γ_{15} (F_{1u}) $\Delta_5^{(2)}$ $[\vec{q}\parallel(\zeta,0,0)]$ or $[\vec{q}\parallel(0,0,\zeta)]$ Σ_4 $[\vec{q}\parallel(\zeta,0,\zeta)]$	Γ_5 (E) Δ_2 $[\vec{q}\parallel(\zeta,0,0)]$ $\Lambda_5^{(2)}$ $[\vec{q}\parallel(0,0,\zeta)]$	Γ_3 (B_2) Σ_2 $[\vec{q}\parallel(\zeta,0,\zeta)]$ Λ_3 $[\vec{q}\parallel(\zeta,0,\bar{\zeta})]$ τ_2 $[\vec{q}\parallel(\zeta,0,0)]$	
[001] correlation direction or soft-mode polarization [(001) diffuse planes]	Γ_{15} (F_{1u}) $\Delta_5^{(2)}$ $[\vec{q}\parallel(\zeta,0,0)]$ or $[\vec{q}\parallel(0,\zeta,0)]$ Σ_4 $[\vec{q}\parallel(\zeta,\zeta,0)]$			

polarized along the [001] axis is frozen into static displacements; this component of the ferroelectric mode is stiffened in the tetragonal phase (A_1 mode). Consequently, the crystal distorts and a spontaneous polarization appears along the [001] direction; the [001] correlation and the (001) planes of high x-ray scattering intensity disappear. In the tetragonal phase, strong correlations remain in the [100] and [010] directions and the components of the ferroelectric mode along these directions remain soft (doubly degenerate E mode). The TA and ferroelectic TO branches of Δ_2 and Λ_5 symmetry, polarized along these directions, are low lying and flat. At the tetragonal-orthorhombic phase transition, in the same way, the [100] component of the F_{1u} cubic ferroelectric mode is stiffened giving rise to a permanent electric dipole along the [100] axis, so that the spontaneous polarization turns from the [001] to the [101] pseudocubic direction. The crystal cell elongates along the [100] direction and the [100] correlation disappears. In the orthorhombic phase, the remaining soft component is the B_2 mode polarized along the [010] axis. The correlation along this direction gives rise to low-frequency branches and to the (010) diffuse planes. Finally, in the rhombohedral phase, all anomalies disappear with the condensation of the B_2 mode. All these aspects are summarized in Table III.

VI. CONCLUSION

The anomalies observed in $KNbO_3$ such as the diffuse x-ray scattering planes and the high anisotropy of the TA and ferroelectric TO branches can be explained by the existence of strong correlations related to the soft $q=0$ modes. Such anomalies were also observed in $KTaO_3$,[18,19] and KTN [$K(Ta:Nb)O_3$],[20,21] to which our description of the ferroelectric phase transition mechanism can be also applied. The correlations are due to a strong dipole-dipole coupling along the $\langle 100\rangle$ directions, which destabilizes the modes polarized along these directions. At each phase transition, when cooling, a soft component mode is stiffened and an oscillating dipole along the soft eigenvector direction freezes into a permanent dipole.

Another explanation of these phenomena in ABO_3 materials has been given recently by Migoni *et al.*,[22,23] who assume an anisotropy of the oxygen polarizability and a hybridization of the oxygen p states with the d states of the central metal ion. In this case the deformability of the oxygen ion is much higher in the direction of B ions than that in the A-O planes. This is quite consistent with our description of the mechanism of the phase transitions in $KNbO_3$ and is indeed complementary.

ACKNOWLEDGMENTS

The authors wish to thank Dr. G. Metrat for providing the excellent $KNbO_3$ samples used in this study. We are also grateful to D. C. Tennant and to Dr. J. Gallant for expert technical assistance.

APPENDIX: GROUP THEORY OF LATTICE VIBRATIONS IN TETRAGONAL $KNbO_3$

We have used the character tables of the irreducible representations (IR) of the point groups reported by Kovalev[25] for the mode decomposition into the irreducible representations. For determining the form of the eigenvectors corresponding to each IR we have applied the projection operator technique described by Maradudin and Vosko.[27]

A. Character tables

1. $\vec{q}=(0,0,\zeta)$

This case includes the Λ direction ($0<\zeta<\frac{1}{2}$), the Γ point ($\zeta=0$), and the Z point ($\zeta=\frac{1}{2}$). So we use the general τ_i notation; C_i indicates the number of times that a representation τ_i appears in the decomposition.

IR	C_i	K	Nb	$O_{(1)}(z)$	$O_{(2)}(y)$	$O_{(3)}(x)$
τ_1	4	0,0,α	0,0,β	0,0,γ	0,0,δ	0,0,δ
τ_3	1	0,0,0	0,0,0	0,0,0	0,0,δ	0,0,$-\delta$
$\tau_5^{(2)}$	5	α,0,0	β0,0	γ,0,0	δ,0,0	ϵ,0,0
	5	0,α,0	0,β,0	0,γ,0	0,δ,0	0,ϵ,0

In the chemical notation, for the Γ point, τ_1, τ_3, and τ_5 correspond respectively to A_1, B_1, and E.

2. $\vec{q}=(\zeta,\zeta,0)$, Σ *direction*

IR	C_i	K	Nb	$O_{(1)}(z)$	$O_{(2)}(y)$	$O_{(3)}(x)$
Σ_1	9	α,α,α'	β,β,β'	γ,γ,γ'	δ,ϵ,δ'	ϵ,δ,δ'
Σ_2	6	$\alpha,-\alpha,0$	$\beta,-\beta,0$	$\gamma,-\gamma,0$	$\delta,-\epsilon,\delta'$	$\epsilon,-\delta,-\delta'$

3. $\vec{q}=(\zeta,0,0)$, Δ *direction*

IR	C_i	K	Nb	$O_{(1)}(z)$	$O_{(2)}(y)$	$O_{(3)}(x)$
Δ_1	10	$\alpha,0,\alpha'$	$\beta,0,\beta'$	$\gamma,0,\gamma'$	$\delta,0,\delta'$	$\epsilon,0,\epsilon'$
Δ_2	5	0,α,0	0,β,0	0,γ,0	0,δ,0	0,ϵ,0

4. $\vec{q}=(\frac{1}{2},0,0)$, *X point*

IR	C_i	K	Nb	$O_{(1)}(z)$	$O_{(2)}(y)$	$O_{(3)}(x)$
X_1	5	α,0,0	0,0,β	0,0,γ	0,0,δ	ϵ,0,0
X_2	2	0,α,0	0,0,0	0,0,0	0,0,0	0,ϵ,0
X_3	5	0,0,α	β,0,0	γ,0,0	δ,0,0	0,0,ϵ
X_4	3	0,0,0	0,β,0	0,γ,0	0,δ,0	0,0,0

5. $\vec{q} = (\frac{1}{2}, \frac{1}{2}, 0)$, *M point*

IR	C_i	K	Nb	$O_{(1)}(z)$	$O_{(2)}(y)$	$O_{(3)}(x)$
M_1	3	0,0,0	0,0,β	0,0,γ	$\delta, \delta', 0$	$\epsilon, \epsilon', 0$
M_2	1	0,0,0	0,0,0	0,0,0	$\delta, \delta', 0$	$\epsilon, \epsilon', 0$
M_3	1	0,0,0	0,0,0	0,0,0	$\delta, \delta', 0$	$\epsilon, \epsilon', 0$
M_4	2	0,0,α	0,0,0	0,0,0	$\delta, \delta', 0$	$\epsilon, \epsilon', 0$
$M_5^{(2)}$	4	$\alpha, \alpha, 0$	$\beta, \beta, 0$	$\gamma, \gamma, 0$	0,0,δ	0,0,δ
	4	$\alpha, -\alpha, 0$	$\beta, -\beta, 0$	$\gamma, -\gamma, 0$	0,0,δ	0,0,$-\delta$

B. Compatibility relations

1.

Γ		Δ		X
$\Gamma_1^{(4)}$	→	$\Delta_1^{(10)}$	←	$X_1^{(5)} + X_3^{(5)}$
$\Gamma_3^{(1)}$				
$\Gamma_5^{(10)}$	→	$\Delta_2^{(5)}$	←	$X_2^{(2)} + X_4^{(3)}$

2.

Γ		Σ		M
$\Gamma_1^{(4)}$	→	$\Sigma_1^{(9)}$	←	$M_1^{(3)}+M_4^{(2)}+M_5^{(4)}$
$\Gamma_5^{(10)}$				
$\Gamma_3^{(1)}$	→	$\Sigma_2^{(6)}$	←	$M_2^{(1)}+M_3^{(1)}+M_5^{(4)}$

3.

Γ		Λ		Z
$\Gamma_1^{(4)}$	→	$\Lambda_1^{(4)}$	←	$Z_1^{(4)}$
$\Gamma_3^{(1)}$	→	$\Lambda_3^{(1)}$	←	$Z_3^{(1)}$
$\Gamma_5^{(10)}$	→	$\Lambda_5^{(10)}$	←	$Z_5^{(10)}$

[1] A. W. Hewat, J. Phys. C 6, 2559 (1973).
[2] R. Comes, M. Lambert, and A. Guinier, Acta Crystallogr. A 26, 244 (1970).
[3] W. Cochran, Adv. Phys. 9, 387 (1960).
[4] A. Huller, Solid State Commun. 7, 589 (1969).
[5] A. Huller, Z. Phys. 220, 145 (1969).
[6] M. D. Fontana, C. Carabatos, G. Metrat, and G. Dolling, Solid State Commun. 28, 887 (1978).
[7] E. Wiesendanger, Ferroelectrics 6, 263 (1974).
[8] M. D. Fontana, G. E. Kugel, G. Metrat, and C. Carabatos (unpublished).
[9] A. C. Nunes, J. D. Axe, and G. Shirane, Ferroelectrics 2, 231 (1971).
[10] F. X. Winter, E. Wiesendanger, and R. Claus, Phys. Status Solidi B 64, 95 (1974).
[11] T. Fukumoto, A. Okamoto, T. Hattori, A. Mitsuishi, and T. Fukuda, Solid State Commun. 17, 427 (1975).
[12] D. G. Bozinis and J. P. Hurrell, Phys. Rev. B 13, 3109 (1976).
[13] A. M. Quittet, M. I. Bell, M. Krauzman, and P. M. Raccah, Phys. Rev. B 14, 5068 (1976).
[14] R. Currat, R. Comes, B. Dorner, and E. Wiesendanger, J. Phys. C 7, 2521 (1974).
[15] C. H. Perry, H. Buhay, A. M. Quittet, and R. Currat, in *Lattice Dynamics,* edited by M. Balkanski (Flammarion, Paris, 1978), p. 677.
[16] M. P. Fontana and C. Razzetti, Solid State Commun. 17, 377 (1975).
[17] J. C. Slater, Phys. Rev. 78, 748 (1950).
[18] R. Comes, F. Denoyer, and M. Lambert, J. Phys. (Paris) 32, C5-195 (1971).
[19] R. Comes and G. Shirane, Phys. Rev B 5, 1886 (1972).
[20] G. Zaccai and A. W. Hewat, J. Phys. C 7, 15 (1974).
[21] W. B. Yelon, W. Cochran, G. Shirane, and A. Linz, Ferroelectrics 2, 261 (1971).
[22] R. Migoni, H. Bilz, and D. Bäuerle, Phys. Rev. Lett. 37, 1155 (1976).
[23] R. Migoni, H. Bilz, and D. Bäuerle, in *Lattice Dynamics,* edited by M. Balkanski (Flammarion, Paris, 1978), p. 650.
[24] R. A. Cowley, Phys. Rev. 134, A981 (1964).
[25] O. V. Kovalev, *Irreducible Representations of the Space Groups* (Gordon and Breach, New York, 1964).
[26] C. J. Bradley and A. P. Cracknell, *The Mathematical Theory of Symmetry in Solids* (Clarendon, Oxford, 1972).
[27] A. A. Maradudin and S. H. Vosko, Rev. Mod. Phys. 40, 1 (1968).